AIAA 2003–6549

Development and Flight Testing of Flapping-Wing Propelled Micro Air Vehicles

Kevin D. Jones, Chris J. Bradshaw,
Jason Papadopoulos and Max F. Platzer
Department of Aeronautics & Astronautics,
Naval Postgraduate School, Monterey, CA 93943

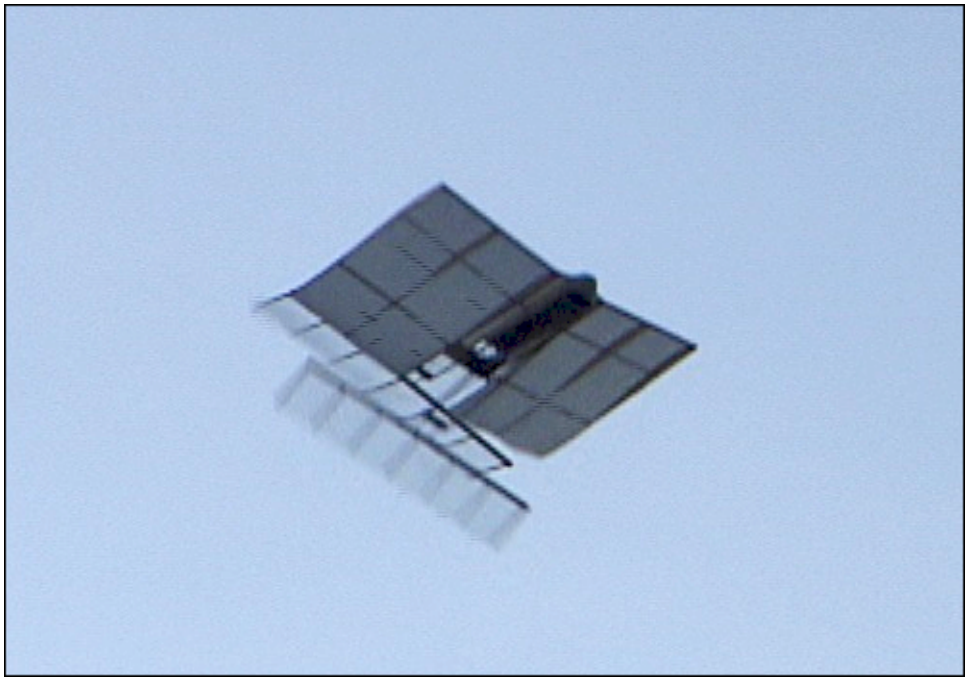

2nd AIAA Unmanned Unlimited Systems, Technologies, and Operations (Aerospace, Land, and Sea) Conference and Workshop
September 15–18, 2003/San Diego, CA

Development and Flight Testing of Flapping-Wing Propelled Micro Air Vehicles

Kevin D. Jones,* Chris J. Bradshaw,† Jason Papadopoulos‡ and Max F. Platzer§
Department of Aeronautics & Astronautics, Naval Postgraduate School, Monterey, CA 93943

In this paper the development and flight testing of flapping-wing propelled, radio-controlled micro air vehicles are described. The vehicles consist of a fixed-wing and a pair of flapping wings immediately downstream of the fixed-wing which flap in counterphase to provide a mechanically and aerodynamically balanced platform and increased efficiency. The models weigh as little as 13 grams, with a 27cm span and 18cm length and will fly for about 20 minutes on a 135 mAh Li-Poly battery. Stable flight at speeds between 2 and 5m/s has been demonstrated, and the models are essentially stall-proof while under power due to the flow-entrainment effect of the flapping-wing pair.

Introduction

THE brilliant success of birds, insects and mammals which achieve flight using flapping-wing propulsion has been an inspiration to humankind for hundreds if not thousands of years. It is sometimes posed that natural selection has led to *optimized* designs; however, it would be naive to assume that what we see in nature are truly the best possible solutions. While the optimization inherent in any evolutionary process cannot be denied, the initial conditions and constraints of an organic creature must be considered. For example, one does not find many rotating parts in nature, and therefore it may be argued that nature did not *select* flapping wings *over* propellers, but rather propellers were excluded from the process entirely. That being said, nature greatly exceeds our expectations in many cases. Gray's paradox and the flight of the bumble-bee are classic examples. Clearly we can learn much from these *less intelligent* but extremely capable creatures.

While historically there has been only limited engineering interest in flapping-wing flight, recent interest in micro air vehicles (MAVs) has led to a renewed interest in the topic and a corresponding influx of research funds. In particular, flapping-wing propulsion has been suggested as an alternative to rotary-wing vehicles, where low-speed or hovering flight is required. Over the past few years, several projects, including the present one, were supported by DARPA, NRL and other government agencies, leading to the development of the rather unconventional flapping-wing propelled MAV shown in Fig. 1.

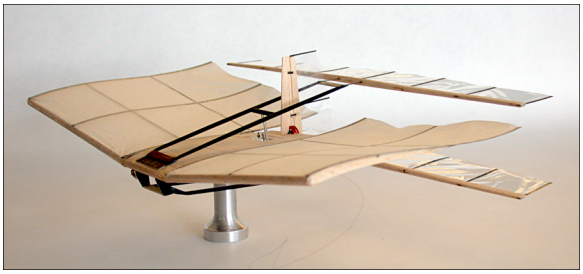

Fig. 1 NPS Flapping-Wing MAV.

Flapping-wing model aircraft date back at least to 1874, when Alphonse Penaud built a rubber-band powered ornithopter. Since then, with just a few exceptions, almost all successful flapping-wing aircraft have been based on a bird-like morphology, at least for the flapping-wings. Probably the most publicized biomimetic flapper is AeroVironment's *Microbat*, shown in Fig. 2. Their philosophy was to take a functional rubber-band powered design and substitute an electrical motor drive train for the rubber-band and add a radio for control.[1] They make an interesting note, stating that the specific energy of the rubber-band is comparable to that of the motor/gearbox/battery/DC-DC-converter assembly. The latest rendition of the Microbat uses a 2-cell Lithium-polymer (Li-poly) battery, three channel radio, and with a 9-inch span and 14 gram total weight, it has made 25 minute flights.

Projects like the Microbat clearly demonstrate that mimicking bird morphology can lead to success, but one is left to ponder whether or not there is a better way. For example, model airplane enthusiasts have been building rubber-band powered ornithopters for more than a century, and to date, the greatest duration was achieved by something that did not look at all like a bird, using instead a biplane flapping mechanism, as shown in Fig. 3. The biplane or *X-wing* canard flapper,

*Research Associate Professor, AIAA senior member.
†Ensign USNR
‡Ensign USNR
§Distinguished Professor, AIAA Fellow.

built in 1985 by Frank Kieser, set a new record for indoor free flight duration.[2] Variations of this design still hold the record.

Following that same direction, a collaboration between SRI and the University of Toronto developed the *Mentor*, shown in Fig. 4, reportedly the first flapping-wing aircraft to hover under its own power.[3] Like Frank Kieser's design, the Mentor is designed to capitalize on the Weis-Fogh or *clap-and-fling* effect, and seems to be designed primarily for hovering flight — a flapping-wing helicopter of sorts, although forward flight has also been demonstrated. Both designs exploit a facet of animal flight technique, the Weis-Fogh effect, but they do it in a way that is quite different than we see in nature; going one step further than biomimicry.

Similarly, we have found it instructive to try to discern which aspects of animal morphology evolved as a result of organic limitations, and which aspects are performance enhancing. One approach we have found useful is to look at how animal behavior is used to compensate for design limitations. For example, birds have evolved with a single pair of wings, so configurations such as the model shown in Fig. 3 are not possible. However, observations of bird flight low over the ocean indicate that birds have indeed discovered the benefits of flapping in ground effect, and this is one of the behavioral adaptations that is exploited in this investigation.

For the present design, much of the development process has been documented over the years in AIAA papers and other publications. A fairly detailed summary of past work can be found in Jones and Platzer,[4] with references to most of our other publications. In this paper the history is briefly summarized, with more details provided on progress made since the earlier publications, and some summarizing remarks on what the future might bring.

Design Philosophy

As previously mentioned, much can be learned from observations of animal flight, but care must be taken to determine which features have evolved to enhance performance, and which were forced due to organic or environmental constraints. For example, a bird flaps its wings such that the flap-amplitude varies along the span. This does not appear to be an optimal arrangement, but the bird does not have an alternative. We would prefer to flap the wing with a constant amplitude to produce thrust from the root section of the wing, and to provide for a more efficient span loading.

In the early years of our research, significant effort was directed toward simulations of fairly basic flapping-wing mechanics in an effort to better understand the complicated unsteady flow phenomena, and with the hope of developing numerical tools to aid in a design optimization methodology. Unsteady panel

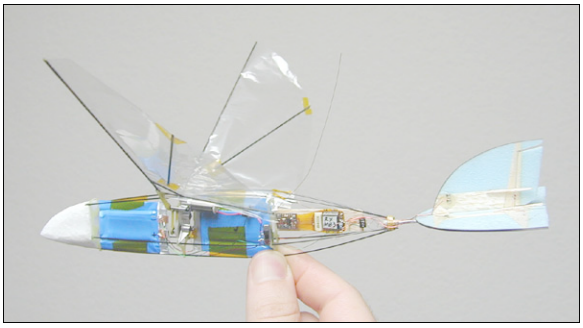

Fig. 2 AeroVironment's Microbat.

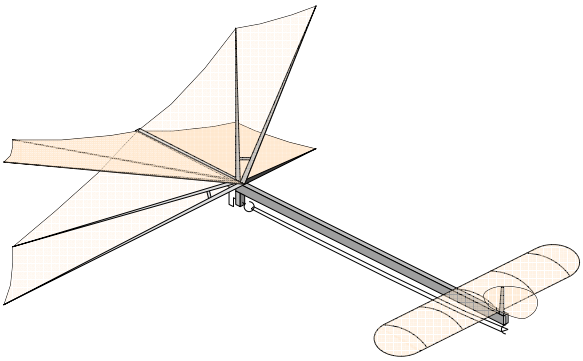

Fig. 3 Frank Kieser's winning *X-wing* flapper.

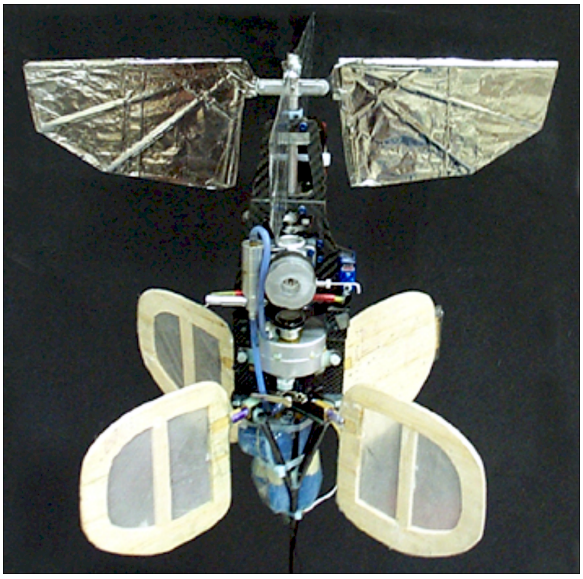

Fig. 4 SRI/UTIAS Mentor flapper.

methods were developed in conjunction with flow visualization and laser Doppler velocimetry (LDV) measurements in wind and water tunnels, and several significant conclusions were made.

First, the benefit of flapping in ground effect was quantified, both numerically and experimentally, as shown in Figs. 5 and 6. For these simulations, an airfoil was plunged sinusoidally at zero angle of attack, with the specified frequency, and with a plunge amplitude of $0.4c$. The ground-effect simulations were modeled using an *image* airfoil below ground, with a mean sep-

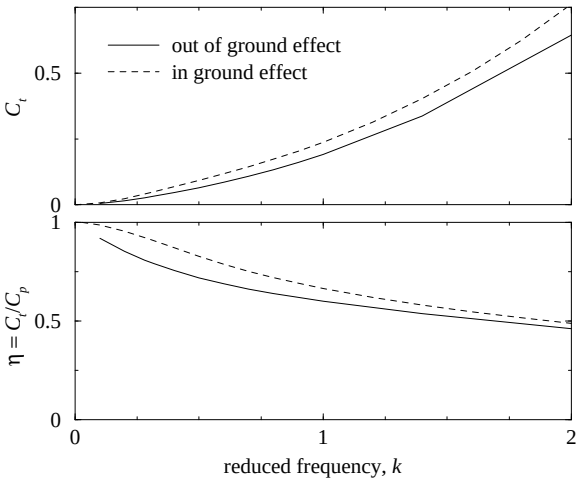

Fig. 5 Predicted benefits of ground effect.

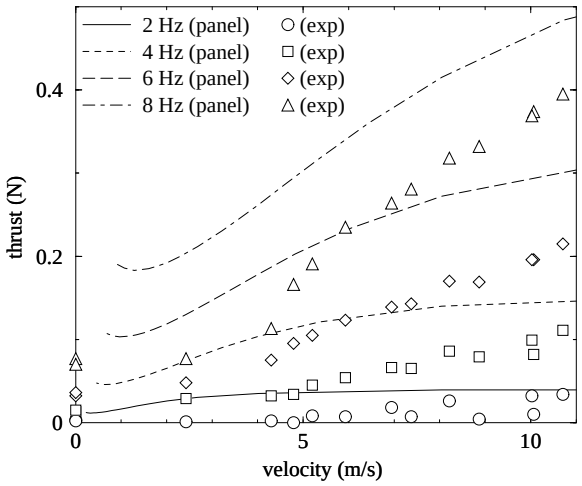

Fig. 6 Thrust measurements in ground effect.

aration of $1.4c$, corresponding to a mean distance from the ground of $0.7c$. The experimental measurements were performed on a biplane model, where the two wings flapped in counterphase, essentially duplicating the panel-code model — emulating ground effect through symmetry.

A secondary benefit of the biplane arrangement was that the model, as a whole, was dynamically balanced, minimizing vibrations of the apparatus. While dynamic balancing was convenient for testing in a wind-tunnel, it appeared to be even more advantageous for a flying model. Flapping a single wing in flight would result in oscillations of the fuselage — work spent with no gain in performance. However, by flapping two wings in counterphase, the fuselage would remain steady, and all the work would be used to move components which directly produce thrust.

It is likely that birds have evolved to compensate for this imbalance. Their neck is highly articulated, such that their head is inertially stable for improved vision, and their body and tail most likely create additional thrust as they oscillate in opposition to the wing flapping. However, it is doubtful that any man-made ornithopters benefit from fuselage oscillations, as this requires a level of sophistication beyond our current capabilities.

Another aerodynamic phenomenon we wished to exploit was the ability to suppress flow separation using the flapping wings. Dynamic stall delay due to oscillatory pitching is a fairly well known phenomenon, of particular interest to rotary-wing engineers. However, a lesser known application is the use of a flapping wing downstream of a larger airfoil, using the favorable pressure gradient of the flapping wing to suppress flow separation on the larger wing. Water-tunnel experiments demonstrated this phenomenon for flow over a backward-facing step,[5] and for separation control of flow over several blunt trailing edge airfoils,[6] and it was hoped that a similar success might be realized on a flapping-wing MAV. This facet is of particular interest for low speed MAVs, as the flight Reynolds numbers may be quite low, on the order of 2×10^4, where the flow is laminar, and separation is likely.

These considerations led us to the configuration shown in Fig. 1, with a biplane-pair of trailing wings, flapping in counterphase, coupled with a large fixed wing located just upstream of the flapping wings.

Design Methodology

As previously mentioned, the early years of our research were focused on developing simulation software which might be used in an optimization algorithm to design an efficient flapping-wing MAV. Unfortunately, what our research demonstrated was that the low Reynolds numbers led to flow physics which could not be adequately predicted using inexpensive methods such as our panel code. Simulations with a two-dimensional unsteady Navier-Stokes solver provided much better agreement with experimental measurements,[7] but were far too costly to be embedded as part of an iterative design process. Therefore, in the end we had to resort to a more hands-on or heuristic approach, using failures and successes to drive the evolutionary design process.

Mechanics of Thrust Generation

One of the first lessons to be learned was simplicity in design. On a large model complicated mechanisms could be developed to add several degrees of freedom to a flapping mechanism. However, working on a MAV-scale, size and weight issues dominated, and the flapping mechanism had to be reduced to a single active degree of freedom — plunge. Test models, like the one shown in Fig. 7 were assembled, allowing for the direct measurement of thrust, and it quickly became apparent that a pitch degree of freedom was necessary, and to keep things simple, this was done passively by attaching the flapping wings to the flapping mechanism with a flexible joint so that they were able to

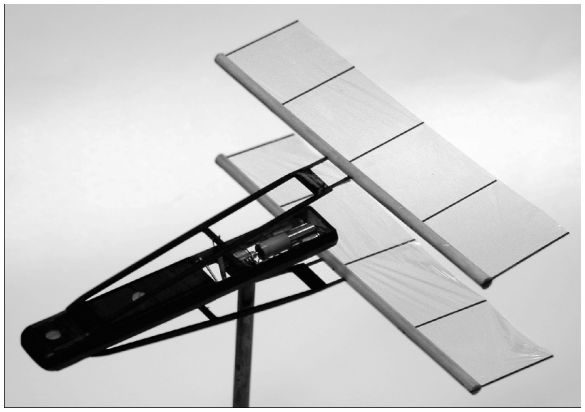

Fig. 7 15cm length/span MAV propulsion model.

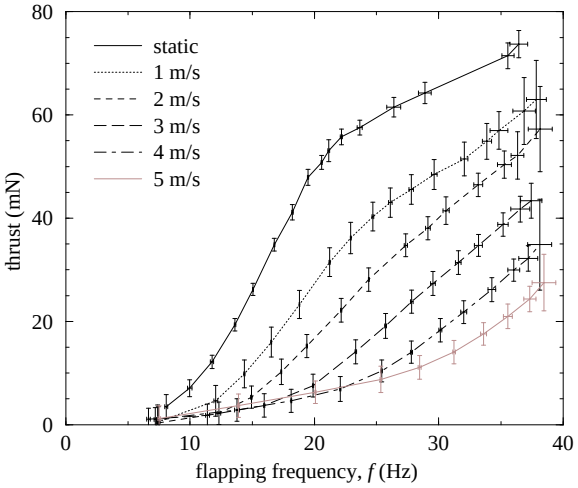

Fig. 8 Performance of the propulsion model.

pitch aeroelastically. Typical performance from the models is shown in Fig. 8.

Inspired by Cylinder *et al.*,[8] a second passive degree of freedom was attempted — camber. The model is shown in action in Fig. 9, with the flash-frozen wings shown at mid-stroke as they pulled away from each other. An elastic angle of attack of about 30 degrees is visible, as well as the wing camber. The performance of the cambering wings is shown in Fig. 10. While the camber provided excellent, and predictable performance for lower frequencies, aeroelastic tuning issues came into play at the higher frequencies. It is likely that these tuning issues can be resolved, but due to the added weight and complexity of the cambering wings, for the time being they were shelved.

With refinements to the design, thrusts of greater than 10 g were realized, and a model equipped with tail fins demonstrated vertical flight, as shown in Fig. 11. All of these models used tiny, geared stepping motors, which required large external power supplies and controllers. While these drive systems were desirable for wind-tunnel models, they were not suitable for flying models, and they were replaced by brushed DC motors with custom gearboxes for the following models.

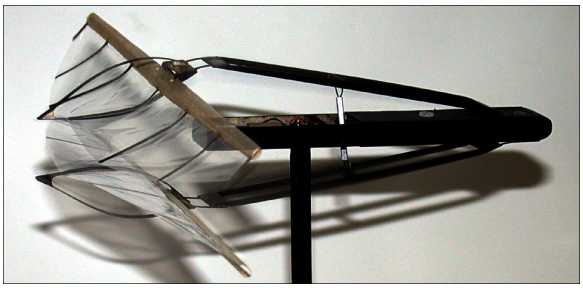

Fig. 9 Aeroelastic cambering wings.

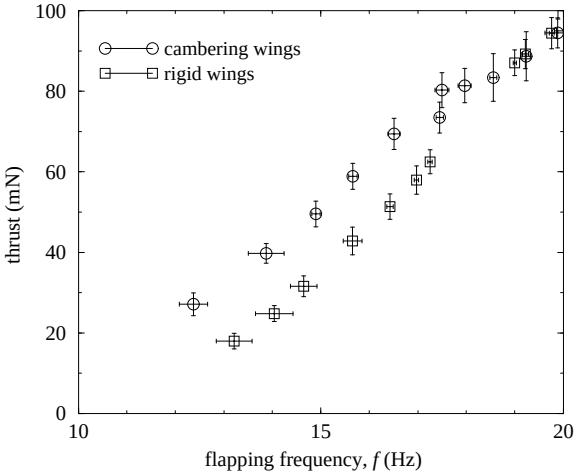

Fig. 10 Static performance of cambering wings.

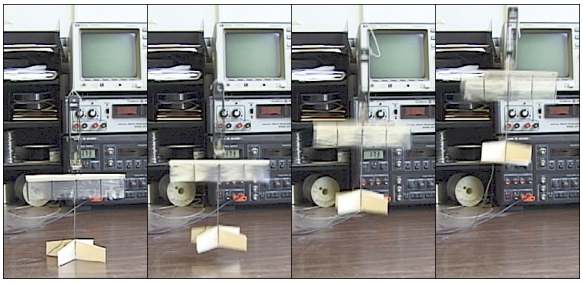

Fig. 11 Vertical takeoff MAV.

Lift Generation

The next step was the integration of the flapping-wing pair with a fixed leading wing. The first test model, shown in Fig. 12, still conformed with DARPA's 15 cm square size criteria. This model was tested in the wind-tunnel, and using flow visualization with a smoke wire, provided the first evidence of separation control using the flapping wings. This is illustrated in Fig. 13, where the wings are not flapping on the left, with the flow separating at the leading edge, and on the right, with the wings flapping, the flow appears to have reattached.

Energy Storage

We are fortunate that some of the critical components we use are also critical to the cell-phone industry, and hence performance improvements have been tremendous. Specifically, batteries, motors (the mo-

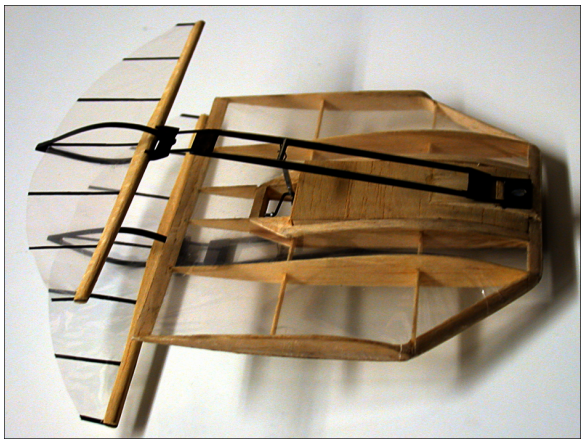

Fig. 12 First fixed/flapping-wing configuration.

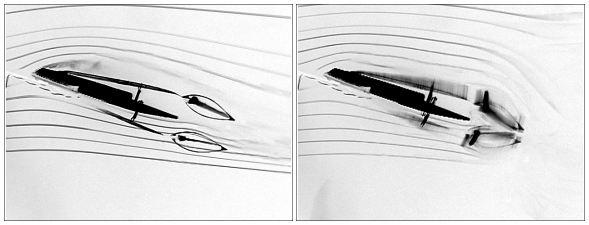

static dynamic

Fig. 13 Separation control at high AOA.

tors that vibrate pagers and cell-phones), and DC-DC converters to step-up a low voltage.

Battery technology has been driven by the cell-phone industry at an extreme pace. Five years ago, about the best solution was a 50 mAh Nickel Cadmium cell, providing 0.06 Wh in a 3.5 g cell — an energy density of about 17 Wh/kg. The rechargeable Li-poly cells we use now have a capacity of 135 mAh and can provide 0.5 Wh. Weighing a mere 3 g, they have an energy density of about 170 Wh/kg, or 10 times what the NiCd cell provided.

Motor/Gear Assembly

The motors are currently the weakest link. While the cell-phone industry has pushed hard to make small, light and cheap motors, they have done little to improve the efficiency. The motors we use weigh about 1.5 g, and use a 2-stage gear system built for the model aircraft hobbyist. Using a custom dynamometer we measured the efficiency of the motor/gear assembly, and at flight loads it is below 25 percent.

On the other hand, the motor/gear assemblies are very light, about 2.5 g, and they can deliver about 0.4 W of shaft power, a power density of 160 W/kg, which is quite good for this scale.

Power Conversion

The motors are really designed for 1.2 V, however to reach the needed power density, we drive them at 5 V using a DC-DC step-up circuit to bump the 3.7 V from the battery up to a regulated 5 V. The circuit is based on an IC designed for cell-phone type devices, but has been miniaturized as much as possible, with some sacrifice in efficiency. The circuit weighs about 0.35 g, and produces a regulated 5 V supply up to about 0.5 A.

Avionics

The radio gear is Current-Off-The-Shelf (COTS) hobbyist equipment, designed for park-flyers and indoor model aircraft. The three channel receiver weighs about 2 g, slightly less if you remove the bulky connector pins it comes with, and it includes an electronic speed control and drivers for two magnetic actuators. The receiver is not narrow band, and is limited to about 100 m range.

The magnetic actuators are comprised of small coils and a magnet pair. The coil is glued to the aircraft frame, and the magnets are glued to the control surface, such that they are inside the coil. When the coil is energized, the magnets try to align with the coil field, deflecting the control surface. If the control surface is lightly spring loaded to return to center, then proportional control can be achieved by varying the duty cycle of the coil. The actuators are not light, 1 g each, and they are not efficient, drawing as much as 0.5 W each, but they are cheap, easy to use and quite durable.

Vehicle Sizing

The next step in the design procedure was to size the configuration for the required payload, in this case, just the propulsion and control system. The components we used on our first model were slightly heavier than those listed above, adding up to about 9.25 g for a battery, converter, drive system and receiver. From past building experience, we estimated the weight of the structure to be about 5 g, yielding a total weight of just over 14 g.

While little experimental data was available for low aspect-ratio wings in the 2×10^4 to 5×10^4 Reynolds number range, papers by Laitone[9] and Torres and Mueller[10] suggested that lift coefficients on the order of about 0.6 were possible with an L/D_{max} of around 5 on an aspect-ratio 2 wing. This indicated that a wing area of about 0.06 m^2 was needed.

Design Evolution

The first model, shown in Figs. 14 and 15, flew in December of 2002. It had a main wing with a 30 cm span and 14.5 cm chord, and flapping wings with a 25 cm span and 4 cm chord. It used a single-channel control, throttle-only, with fixed rudder trim for a shallow turn, and fixed pitch trim to give it a constant nose-up attitude. The flying weight was about 14.4 g, and the model made a number of flights, the longest lasting about 3 minutes before perching in a tree.

Flight speed was only about 2 m/s, and the ability of the model to fly at very high angles of attack without stalling suggested that separation control was in

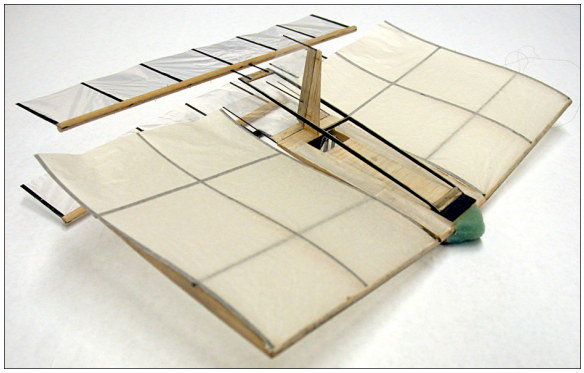

Fig. 14 First flying model.

effect. With the power off, the model would stall quite easily in response to gusts, but under power, it would merely settle back into level flight without loosing any altitude.

Several months later a second model was built, shown previously in Fig. 1 and in flight in Fig. 16. This model was slightly smaller, with a 27 cm span, and included a rudder control. The weight was reduced to 13.4 g, and the model could now sustain longer flights, as trees and buildings could be avoided. During an AIAA technical seminar at NASA Ames on February 12, 2003, the model was flown in the test section of the 80 by 120 foot NFAC tunnel — certainly the cleanest air one could find.

The second model still had no elevator control, so it was trimmed with a nose-up attitude, and throttle was used to control rate-of-climb. By changing the pitch trim, the flight speed could be adjusted. The model flew well from speeds as low as 2 m/s up to about 5 m/s. Higher speeds would be possible with active pitch control, but were risky with a preset pitch trim, as the model might easily dive into the ground in response to a gust.

A Watt-meter was attached to the model on the benchtop, and at full power 1.5 W was drawn from the battery while the model produced about 10 g of static thrust. Considering only the motor/gear efficiency (ignoring losses through the DC-DC converter, receiver/speed-controller, and crankshaft assembly), this suggests that 0.375 W shaft power were delivered, resulting in a figure of merit (FOM) of about 30 g/W at an effective *disk-loading* of about 6 N/m^2.

Design Analysis

With a flying model in hand, we now went back to the wind-tunnel in order to gain a better understanding of the flow physics; hopefully allowing us to optimize the design. Since the pager motors used in the flying model had a relatively short lifespan, a model was built with the same fixed and flapping-wing geometry, but with a large fuselage to house a bigger motor and a rotary encoder and with interchangeable parts. The new model, shown in Fig. 17, was attached

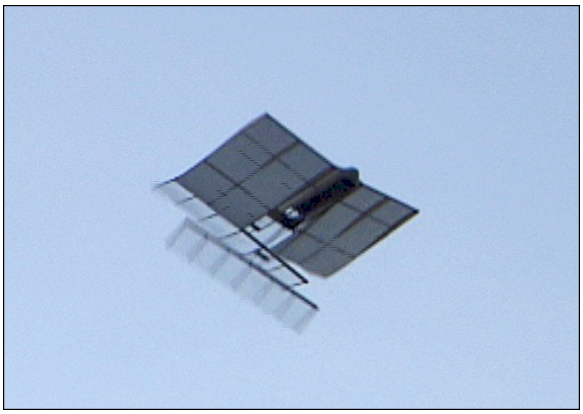

Fig. 15 First model in flight.

Fig. 16 Second model in flight.

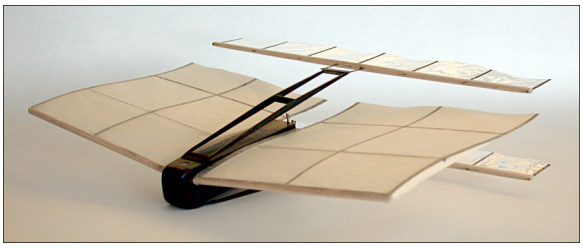

Fig. 17 Wind-tunnel variant of the MAV.

to a 2-component force balance to measure lift and thrust, and flow visualization and unsteady LDV experiments were run.

Flow Visualization

A smoke wire was used to generate streaklines; constructed of 0.25 mm diameter NiCr beaded wire, heated by passing a current through it, and using Rosco Fog Juice as the smoke agent. Imagery was recorded using either a digital still camera or a digital video camera with a high shutter speed to freeze the motion of the wings and streaklines. Details of the methods can be found in Jones and Platzer.[4]

Flow visualization experiments were performed with the model mounted at a 15 degree angle of attack, at a flow speed of about 2 m/s, approximating the flight conditions. Initially the flapping wings were at rest,

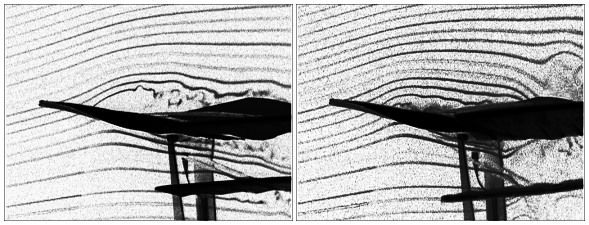

static dynamic

Fig. 18 Separation control at high AOA.

and they were then quickly accelerated to a flapping frequency of about 30 Hz. The results are shown in Fig. 18, viewing the model from the left rear corner forward; an angle which provides a good view of the flow over the upper surface of the left wing. On the left, without wing flapping, it is clearly seen that the flow separates at the leading edge, and the wing is fully stalled. On the right, after just four flapping strokes, the flow is already reattached. While the boundary layer appears to be very thick and unsteady, the outer flow remains parallel to the upper wing surface and reattaches at the trailing edge. Not only is the flow entrainment sufficient to reattach the flow, but it requires only about a tenth of a second to transition. The Reynolds number is about 2×10^4 for the main wing, and just 5×10^3 for the flapping wings.

Laser-Doppler Flow Measurements

A TSI two-channel LDV system with a single probe was used, with flow seeding provided by a Rosco fog generator. For unsteady measurements, the signal from the rotary encoder was fed into a Rotary Motion Resolver (RMR), which allowed the LDV system to record periodic data, synchronized with the wing flapping. Further details about the setup and measurement procedures can be found in Bradshaw.[11]

Use of the RMR provided for higher fidelity velocity measurements, removing the effects of phase-biased flow seeding. Since LDV is a statistical average of a large number of recorded events, in an unsteady, periodic flow, the seeding density may fluctuate periodically, biasing the velocity prediction toward the more heavily seeded parts of the cycle.

To remedy this, using the RMR the flapping cycle was divided into 72 zones, each covering 5 degrees of the flapping cycle, and the average velocity in each zone was measured. By averaging these 72 velocities, the biasing was removed.

This is illustrated in Fig. 19 where the direct (biased) average velocity profile is compared to the average velocity profile predicted using the RMR. The velocities were recorded just downstream of the flapping wings, with the model set at a 15 degree angle of attack, flapping at 32Hz, and with a freestream velocity of 2.75 m/s. While the results are similar, measurements using the RMR tend to resolve higher peaks where flow seeding is typically more diffused.

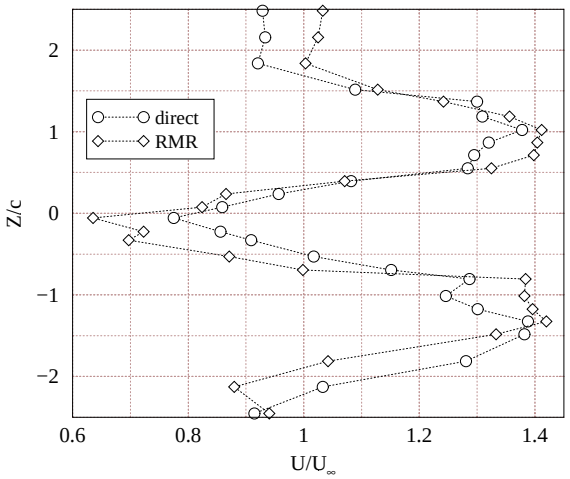

Fig. 19 Time averaging with and w/o the RMR.

The flow-entrainment effect is illustrated in Figs. 20 and 21. In Fig. 20 the time-averaged velocity profile just in front of the flapping wings ($x = 0$) is shown for three cases. In the first case, the main wing is removed, and the wings are flapped at 32Hz. In the second case the main wing is included, but the wings are not flapped. In the third case, the main wing is included and the wings are flapped at 32Hz. In all three cases the freestream speed is 2.75 m/s, and the model is set at a 15 degree angle of attack. Unfortunately, the dihedral of the main wing masked a large area above the symmetry plane, roughly where the figure legend is placed, such that the effect of the upper flapping wing is not visible.

Comparing the flapping cases with and without the main wing, the entrainment effect is clearly seen with about a 30 percent over-velocity at the centerline of the lower flapping wing. Note that the velocity profile is nearly unaffected by the inclusion of the main wing. Without flapping the wings, a large velocity deficit is seen near the stagnation point on the leading edge of the lower flapping wing. Also note that without flapping the wings, a velocity deficit appears more than a chordlength above the main wing, illustrating the severity of the separated flow.

In Fig. 21, velocity profiles a chordlength upstream of the flapping wings ($x = -c$) are shown for the same three cases, and it can be seen that the entrainment effect has diminished considerably, indicating that the flapping wings must be quite close to the trailing edge of the main wing to capitalize on this phenomenon.

Force Measurements

Direct lift and thrust measurements were made using a two component force balance. The balance was attached to a permanent structure fixed to the concrete floor below the tunnel, preventing tunnel vibrations from degrading the results. Several configurations were evaluated over a wide gamut of conditions, however just a few results are included here to il-

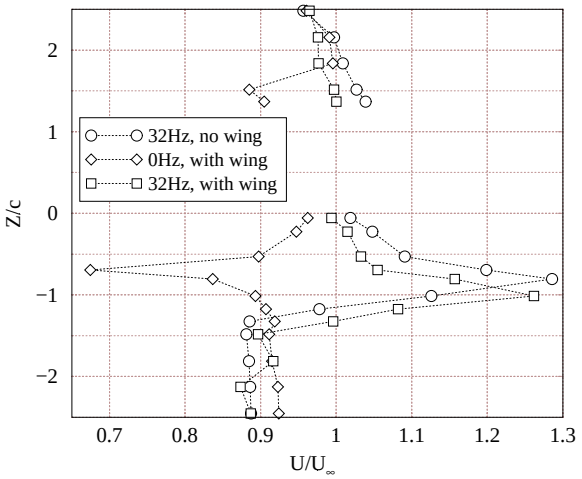

Fig. 20 Time-averaged velocity at $x - 0$.

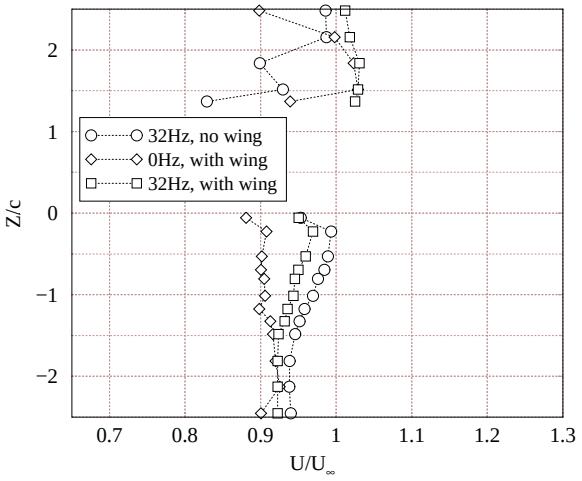

Fig. 21 Time-averaged velocity at $x = -c$.

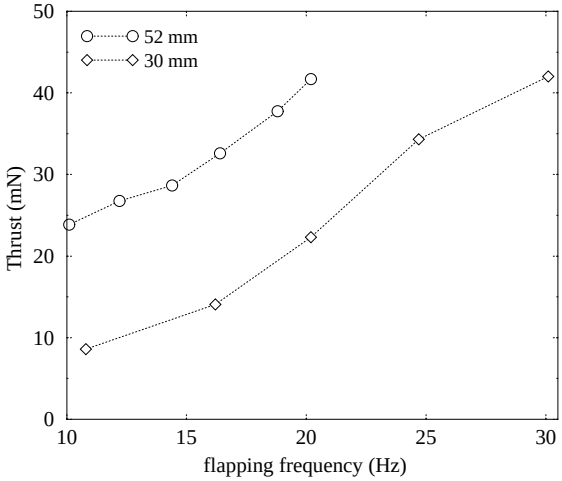

Fig. 22 Effect of wing spacing on thrust.

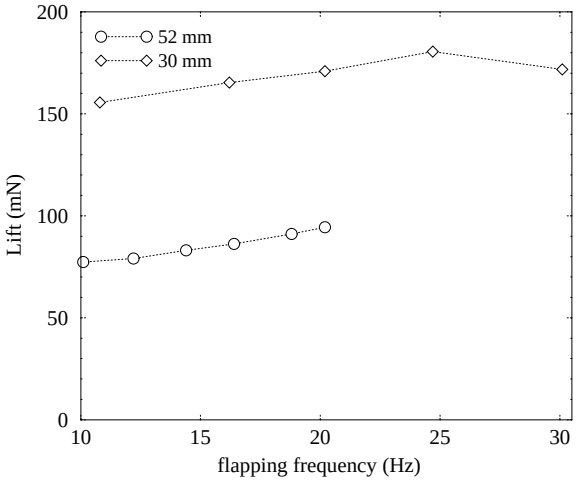

Fig. 23 Effect of wing spacing on lift.

lustrate the flow entrainment effect. The apparatus, measurement procedure and all results are described in Papadopoulos.[12]

The measured thrust and lift are shown in Figs. 22 and 23, respectively, for the on-design model, and for a variation where the minimum spacing between the flapping wings is reduced from 52 mm to 30 mm. The flow speed is 3 m/s, with the models at a 15 degree angle of attack, and the flap-amplitude and all other geometric parameters are the same. Changing the separation between the wings has several effects. It changes the strength of the ground-effect emulation, it changes the aeroelastic behavior of the passive pitching mechanism, and it alters the relationship between the flapping wings and the boundary layer of the main wing.

While there are questions as to the cause, the effect of the change is dramatically visible in Figs. 22 and 23. By reducing the space between the wings, the thrust is significantly reduced, but the lift is significantly increased. One theory is that in the first case the flapping wings transfer momentum into the flow in the form of thrust, and in the second case the momentum is used to reattach the boundary layer, significantly increasing the lift. More work will need to be done to evaluate this phenomenon.

Summary & Prospective

Almost a decade of research in flapping-wing propulsion and low Reynolds number unsteady aerodynamics has culminated in the development of an unusual flapping-wing propelled micro air vehicle. The configuration consists of a biplane pair of flapping wings, which move in counterphase, located just downstream of a fixed wing. The relatively large fixed wing provides most of the lift, while the flapping-wings provide the thrust and suppress flow separation on the main wing due to their flow entrainment. The symmetry of the flapping-wing pair provides mechanical and aerodynamic balancing, and produces thrust more efficiently than conventional flapping-wing systems.

The present model, using *current off the shelf* power and avionics equipment, has a 27 cm span, 18 cm length and weighs a paltry 13.4 g, with two-channel control and enough battery capacity for 15 to 20 minutes of flight. The model does not have active pitch

control, but the pitch may be manually trimmed to control the flight speed. Speeds between about 2 m/s and 5 m/s have been achieved, and the model is virtually stall-proof while under power, due to the separation suppression characteristics of the design.

Wind-tunnel measurements of lift and thrust, as well as flow visualization and unsteady LDV measurements of the surrounding flowfield have verified the flow separation suppression phenomenon, and now provide a means for the systematic analysis of the design, which will eventually allow for design optimization. While the current design flies extremely well, it is by no means optimized. However, operating with a static figure of merit of almost 30 g/W, it greatly surpasses low Reynolds number propeller performance at an equivalent disk loading. Furthermore, the design should scale down well, allowing for much smaller vehicles as power and avionics technology improves.

While there are several natural directions for the project to evolve, its low speed performance makes it highly suitable for missions where flight in confined areas is required. It is likely that the flight speed can be reduced much further, perhaps eventually achieving hovering flight. Along with the low flight speed comes the ability to *park* the vehicle in strategic places, allowing it to gather and transmit data long past its useful flight lifetime. There are certainly many other possibilities, limited only be our creativity and perseverance.

Acknowledgments

We are grateful for the support received from Richard Foch, head of the Vehicle Research Section of the Naval Research Laboratory, and project monitors Kevin Ailinger, Jill Dahlburg and James Kellogg.

References

[1] Keennon, M. T. and Grasmeyer, J. M., "Development of the Black Widow and Microbat MAVs and a Vision of the Future of MAV Design," *AIAA/ICAS International Air and Space Symposium and Exposition—The Next 100 Years*, AIAA Paper No. 2002-3327, July 2003.

[2] Chronister, N., "Ornithopter Media Collection," Published on the web at *indev.hypermart.net/rubber.html*, 2001.

[3] Bridges, A., "Flying Robots Create a Buzz," Monterey County Herald, July 28, 2002.

[4] Jones, K. D. and Platzer, M. F., "Experimental Investigation of the Aerodynamic Characteristics of Flapping-Wing Micro Air Vehicles," *41st Aerospace Sciences Meeting & Exhibit*, AIAA Paper No. 2003-0418, Jan. 2003.

[5] Lai, J. C. S., Yue, J., and Platzer, M. F., "Control of Backward Facing Step Flow Using a Flapping Airfoil," *Experiments in Fluids*, Vol. 32, 2002, pp. 44–54.

[6] Tuncer, I. H., Lai, J. C. S., and Platzer, M. F., "A Computational Study of Flow Reattachment Over a Stationary/Flapping Airfoil Combination in Tandem," *36th Aerospace Sciences Meeting & Exhibit*, AIAA Paper No. 98-0109, Jan. 1998.

[7] Castro, B. M., *Multi-Block Parallel Navier-Stokes Simulations of Unsteady Wind Tunnel and Ground Interference Effects*, Ph.D. thesis, Department of Aeronautics & Astronautics, Naval Postgraduate School, Sept. 2001.

[8] Cylinder, D., Srull, D., and Kellogg, J., "Biomorphic Approaches to Micro Air Vehicles," *UAV Asia-Pacific 2003 Conference*, Feb. 2003.

[9] Laitone, E. V., *Fixed and Flapping Wing Aerodynamics for Micro Air Vehicle Applications*, Vol. 195 of *Progress in Astronautics and Aeronautics*, chap. 5: Wind Tunnel Tests of Wings and Rings at Low Reynolds Numbers, AIAA, 2001, pp. 83–90.

[10] Torres, G. E. and Mueller, T. J., *Fixed and Flapping Wing Aerodynamics for Micro Air Vehicle Applications*, Vol. 195 of *Progress in Astronautics and Aeronautics*, chap. 7: Aerodynamic Characteristics of Low Aspect Ratio Wings at Low Reynolds Numbers, AIAA, 2001, pp. 115–142.

[11] Bradshaw, C. J., *An Experimental Investigation of Flapping Wing Aerodynamics in Micro Air Vehicles*, Master's thesis, Department of Aeronautics & Astronautics, Naval Postgraduate School, June 2003.

[12] Papadopoulos, J. P., *An Experimental Investigation of the Geometric Characteristics of Flapping-Wing Propulsion for a Micro Air Vehicle*, Master's thesis, Department of Aeronautics & Astronautics, Naval Postgraduate School, June 2003.